Organic & Biomolecular Chemistry

Dynamic Article Links

Cite this: *Org. Biomol. Chem.*, 2011, **9**, 5445

www.rsc.org/obc

PAPER

Symmetric dithiodigalactoside: strategic combination of binding studies and detection of selectivity between a plant toxin and human lectins

Sonsoles Martín-Santamaría,[a] Sabine André,[b] Eliza Buzamet,[c,d] Rémi Caraballo,[e] Gloria Fernández-Cureses,[c] Maria Morando,[f] João P. Ribeiro,[f] Karla Ramírez-Gualito,[f] Beatriz de Pascual-Teresa,[a] F. Javier Cañada,[f] Margarita Menéndez,[c,d] Olof Ramström,[e] Jesús Jiménez-Barbero,*[f] Dolores Solís[c,d] and Hans-Joachim Gabius[b]

Received 22nd December 2010, Accepted 21st April 2011
DOI: 10.1039/c0ob01235a

Thioglycosides offer the advantage over O-glycosides to be resistant to hydrolysis. Based on initial evidence of this recognition ability for glycosyldisulfides by screening dynamic combinatorial libraries, we have now systematically studied dithiodigalactoside on a plant toxin (*Viscum album* agglutinin) and five human lectins (adhesion/growth-regulatory galectins with medical relevance *e.g.* in tumor progression and spread). Inhibition assays with surface-presented neoglycoprotein and in solution monitored by saturation transfer difference NMR spectroscopy, flanked by epitope mapping, as well as isothermal titration calorimetry revealed binding properties to VAA (K_a: 1560 ± 20 M^{-1}). They were reflected by the structural model and the affinity on the level of toxin-exposed cells. In comparison, galectins were considerably less reactive, with intrafamily grading down to very minor reactivity for tandem-repeat-type galectins, as quantitated by radioassays for both domains of galectin-4. Model building indicated contact formation to be restricted to only one galactose moiety, in contrast to thiodigalactoside. The tested glycosyldisulfide exhibits selectivity between the plant toxin and the tested human lectins, and also between these proteins. Therefore, glycosyldisulfides have potential as chemical platform for inhibitor design.

Introduction

The growing insights into the molecular basis of physiological processes guide the selection of new targets for drug design. Owing to the unsurpassed capacity of glycans to store biological information, the development of a wide array of respective receptors (lectins) and their dynamic interplay triggering specific cellular responses *e.g.* in growth regulation, the design of compounds that potently interfere with lectin-glycan recognition has become a challenge.[1] Initially mostly addressed for plant lectins such as concanavalin A, the selection is shifting to medically relevant proteins, that is, to distinct biohazardous toxins and human lectins. Technically, the aim of identifying promising anti-lectin lead compounds prompted the introduction of high-throughput screening and diverse types of library approaches.[2] Along these lines, we have targeted on two such classes of galactoside-binding lectins (toxic AB-type lectins, here *Viscum album* agglutinin (VAA), and the family of adhesion/growth-regulatory galectins with its three groups of proto-, chimera- and tandem-repeat-type proteins[3]) and applied the dynamic combinatorial library approach based on thiol-disulfide exchange with thioglycosides.[4] As previously demonstrated, the dynamic library approach is indeed a viable route to identifying new disulfide ligands for lectins.[4d] Nevertheless, the main objective of this study has not been to further explore this methodology, but rather to evaluate the properties of a ligand that was previously identified.

In principle, S-glycosides have the pharmacodynamic advantage of being resistant to hydrolytic cleavage. However, the substitution engenders enhancement of flexibility and alteration of the topology (C–S/C–O bond lengths: 1.78 Å *vs.* 1.41 Å; C–S–C/C–O–C bond angles: 98° *vs.* 117°).[5] These differences from O-glycosides put bioactivity of these derivatives into question. However, by

[a]*Departamento de Química, Facultad de Farmacia, Universidad San Pablo CEU, Boadilla del Monte, 28668, Madrid, Spain*
[b]*Institute of Physiological Chemistry, Faculty of Veterinary Medicine, Ludwig-Maximilians-University Munich, Veterinärstr. 13, 80539, Munich, Germany*
[c]*Instituto de Química Física Rocasolano, Consejo Superior de Investigaciones Científicas, Serrano 119, 28006, Madrid, Spain*
[d]*Centro de Investigación Biomédica en Red de Enfermedades Respiratorias (CIBERES), Bunyola, Mallorca, Illes Balears, Spain*
[e]*Department of Chemistry, KTH-Royal Institute of Technology, Teknikringen 30, 10044, Stockholm, Sweden*
[f]*Chemical and Physical Biology, Centro de Investigaciones Biológicas, Consejo Superior de Investigaciones Científicas, Ramiro de Maeztu 9, 28040, Madrid, Spain*

testing thiodigalactoside (TDG) in inhibition assays, the S-glycosidic bond has been shown to interact with AB-type plant toxins and galectins, with a tendency for an increased entropic penalty compensated by an enthalpic gain relative to lactose in the thermodynamic balance sheet.[6] Moving beyond thioglycosides, the synthesis of glycosyldisulfides had been motivated to make effective glycosyl donors and a new class of test compounds available.[7] In this respect, our screening of disulfide-forming thioglycoside libraries with the toxin from mistletoe had indeed indicated a potential of dithiodigalactoside (DTDG) to protect a human cell line from toxin binding.[4d] Also, the asymmetric disulfide of N-acetylated galactosamine and glucosamine, a derivative of di-*N*-acetylated lactose, appeared to harbour reactivity for galectin-3.[4d] These initial results on bioactivity of a diglycosyldisulfide prompted us to systematically investigate the reactivity profile of DTDG relative to TDG and lactose. In detail, we addressed the following issues:

a.) to determine its binding capacity to the mistletoe toxin in two assay systems of increasing biorelevance,

b.) to provide a structural model for binding, and

c.) to determine the relative reactivity to human galectins from each of the three groups listed above, to build a structural model for a representative complex and to run assays with the two separate domains of a tandem-repeat-type family member, *i.e.* galectin-4.

Technically, ligand properties of the synthetic product were assessed by spectrophotometric and radioactivity-based inhibition assays, epitope mapping and competitive binding analysis in saturation transfer difference (STD) NMR spectroscopy, isothermal titration calorimetry (ITC) and fluorescent cell assays, flanked by computational docking to visualize a model for the formation of lectin-glycosyldisulfide complexes.

Results and discussion

Synthesis

The symmetrical disulfide was obtained in a three-step procedure using a solution of iodine in ethanol in the last step, as outlined in Scheme 1. This compound was used to probe for its ligand properties on the plant toxin in biochemical, ITC, NMR spectroscopical and cell biological assays.

Assaying ligand properties on the toxin

A convenient test method is the analysis of the extent of lectin binding to surface-presented glycans in the absence and presence of compounds examined for inhibitory activity. Using lactose as interaction partner by adsorbing a lactose-bearing neoglycoprotein to the surface of microtiter plate wells, binding of biotinylated VAA was first ascertained to be saturable and blocked by presence of cognate sugar but not mannose or glucose. The dependence on binding the carbohydrate specifically was further substantiated by lack of VAA interaction with a neoglycoprotein constituted by the same carrier protein (bovine serum albumin) but presenting mannose as sugar headgroup. Next, conditions were defined to ensure signal intensity in the linear range by varying the lectin concentration in order to reach optimal sensitivity. The ensuing inhibitory titrations at constant lectin concentration with increasing concentrations of tested compounds resulted in a reduction of the extent of binding of the labelled toxin to the ligand-bearing matrix (Fig. 1). TDG was a slightly more efficient inhibitor than lactose when expressed in the measured IC_{50}-values (Table 1). Thus, the solid-phase inhibition assay was suitable to determine reactivity and to provide a comparative measure. Tested under these conditions, DTDG obviously had inhibitory capacity (Fig. 1). It was about 2–3-fold lower than for TDG (Table 1).

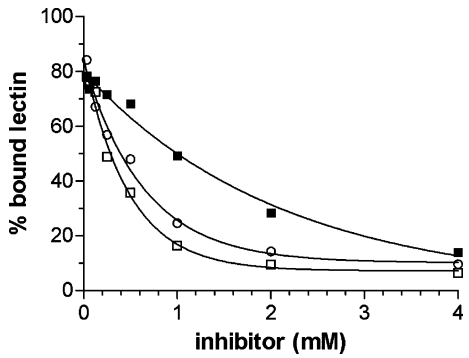

Fig. 1 Titration curves illustrating the course of inhibition of binding of biotinylated VAA (3 μg ml^{-1}) to lactosylated neoglycoprotein in a solid-phase assay by increasing concentrations of thiodigalactoside (□), dithiodigalactoside (■) and lactose (○).

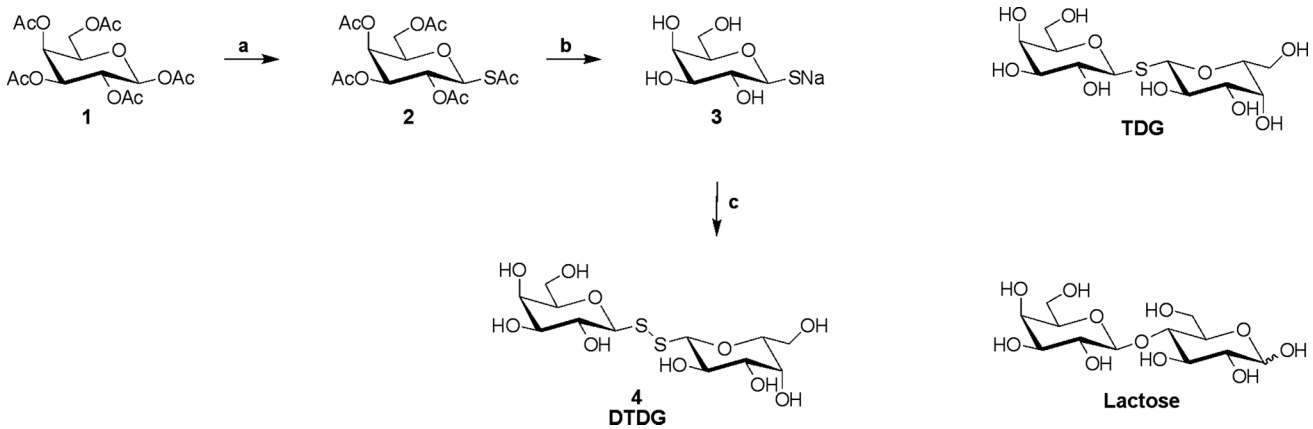

Scheme 1 Reagents and conditions: a) HSAc, $BF_3{\cdot}Et_2O$, CH_2Cl_2, 0 °C - rt, 24 h (89%); b) NaOMe, MeOH, 2 h (97%); c) H_2O, I_2-EtOH.

Table 1 Relative inhibitory potency of lactose (Lac), thiodigalactoside (TDG) and dithiodigalactoside (DTDG) on lectin binding to a surface-immoblized neoglycoprotein (expressed as IC_{50}-value, in mM)[a]

Lectin	Lac	TDG	DTDG
VAA (3 μg ml^{-1})	0.6	0.4	1.1
galectin-1 (20 μg ml^{-1})	0.8	0.5	4.8
galectin-3 (15 μg ml^{-1})	1.6	1.1	5.4
galectin-4 (5 μg ml^{-1})	3.5	1.8	> 10
galectin-7 (30 μg ml^{-1})	4.0	2.3	> 10
galectin-8 (0.1 μg ml^{-1})	1.2	1.4	> 10

[a] Titrations were performed using a constant coating concentration of neoglycoprotein (0.25 μg/well) with eight concentrations of sugar in triplicates and up to six independent series, reaching an upper limit of 13.7% for the standard deviation (for exemplary titration curve, please see Fig. 1).

These results intimated a direct competition between the natural β-galactoside presented by the neoglycoprotein and the tested thiocompounds. To independently verify this assumption we next ran direct competition assays in solution, monitored by STD NMR spectroscopy.

In this setting, lactose was the reporter ligand, whose contact profile, which underlies magnetization transfer from the saturated protein to distinct ligand protons, is known.[8] A reduction of the intensity of these signals of lactose in the presence of an inhibitor reflects the loss of lectin-lactose contact and the relative inhibitory capacity of the tested compound. The respective titrations confirmed the inhibitory activity of DTDG and yielded a relative potency of about 0.5–0.7fold for DTDG when compared to TDG. Since these experiments further documented complex formation with the disulfide, we proceeded to perform isothermal titration calorimetry for direct affinity measurement, using TDG as positive control.

Representative ITC curves for both compounds are shown in Fig. 2A. Titration data obtained with both DTDG and TDG could be fitted to a one-set-of-sites model with association constants, K_a, of 1560 ± 20 M^{-1} (ΔG = −18.16 ± 0.03 kJ mol^{-1}) and 2600 ± 100 M^{-1} (ΔG = −19.4 ± 0.1 kJ mol^{-1}), respectively. A reliable determination of the binding stoichiometry for this range of affinities would require running the titrations at protein concentrations over the natural solubility level of VAA. Therefore, only total estimates of enthalpy/entropy changes per B chain, −50.3 ± 0.4 kJ mol^{-1}/−108 ± 1 J mol^{-1} K^{-1} (DTDG) and −53 ± 1 kJ mol^{-1}/−110 ± 30 J mol^{-1} K^{-1} (TDG), were derived from the analysis. ITC data obtained for lactose under similar conditions[9] were consistent with two sets of sites with K_a of 1.1 × 10^3 M^{-1} and 1.6 × 10^4 M^{-1}, assigned to 2γ (Tyr-sites) and 1α (Trp-sites) subdomains of the B-chains, respectively, the accessibility to the Trp-sites being restricted by tetramer formation. The fact that data obtained for DTDG and TDG could be fitted to a one-set-of-sites model imply that if both Tyr- and Trp-sites are operative for binding the thioderivatives, they must exhibit similar affinities. At any rate, DTDG binds to VAA with lower affinity than TDG.

Having herewith determined the affinity of DTDG to the toxin, STD NMR spectroscopy was used for epitope mapping by recording proton signals of the ligand when separately running experiments with lactose, TDG and DTDG. The primary contact of disaccharides with VAA is the galactose unit, and the penultimate sugar moiety of disaccharides is known to lose its mobility to varying degrees.[10] As exemplarily shown by the strong signals in the case of DTDG (Fig. 3 left), ligand protons at positions 2, 3 and 4 in the galactose pyranose ring appear to be in close vicinity to the protein in all three sugars, irrespective of the nature of the glycosidic bond. This experimental observation agrees with the conclusions derived from chemical-mapping studies,[6i] and can be readily reconciled with the model of the complex obtained by *in silico* docking (Fig. 4). The predicted binding patterns for TDG and DTDG were nearly indistinguishable. Main interactions at the Tyr-sites for both thiocompounds are hydrogen bonds involving hydroxyl groups at positions O3 (with Asp235 and Asn256) and O4 (with Gln238) as well as CH-π interactions of pyranose hydrogens H3, H4 and H5 with Tyr249. The second galactose unit can

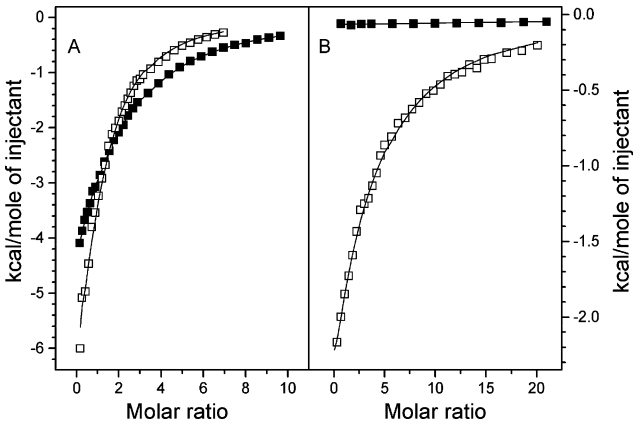

Fig. 2 Calorimetric titration of VAA (A) and human galectin-4 (B) with thiodigalactoside (□) and dithiodigalactoside (■). Representative plots of the heat released per mole of ligand injected in the course of titrations as a function of the sugar/protein molar ratio. Solutions of VAA at 337.5 μM (□)/243 μM (■) (in terms of AB heterodimer concentration) and of galectin-4 at 117 μM (□)/154.7 μM (■) were used in these titrations. Solid lines correspond to the best fit of the experimental data using a one-set-of-sites model.

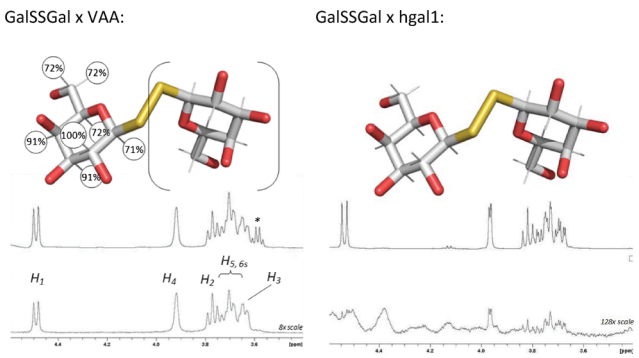

Fig. 3 Illustration of relative STD signal intensities of protons for the galactose moiety of dithiodigalactoside binding to the Tyr site of VAA (left) and to human galectin-1 (right). The 500 MHz off-resonance (above) and the STD (below) spectra are presented in the lower panel. The STD signals (even amplified 128 fold) for the hgal-1 complex are very weak indicating that the binding affinity is very low. This feature strongly contrasts with the observation for the VAA complex (amplified 8 fold). The asterisk denotes the presence of a small amount of ethanol in the sample, which does not give STD signal.

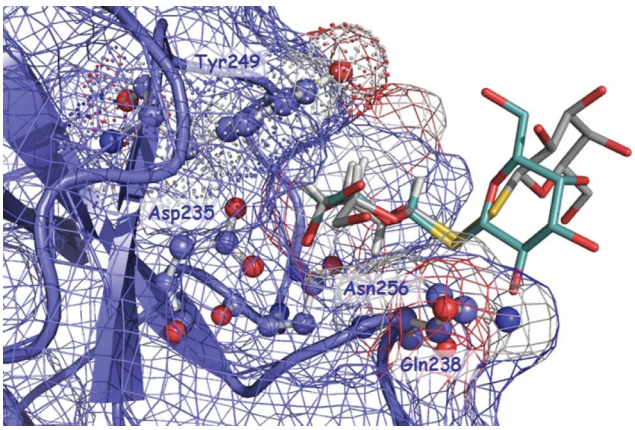

Fig. 4 Structural model of the complex of VAA (Tyr site, surface representation) with thiodigalactoside (green) and dithiodigalactoside (grey), based on docking analysis and the experimental input from STD NMR spectroscopy. While one galactose unit makes several contacts (hydrogen bonds with Asp235 and Asn256, and CH-π interactions with Tyr249 (with its van der Waals surface emphasized by the dots representation)), the second moiety contributes weakly to complex stabilization with Gln238 in the case of TDG. The van der Waals surfaces are emphasized with the grid and the dots.

contact Glu238 as part of TDG but not of DTDG (Fig. 4). After having herewith characterized the ligand properties of DTDG and presented a structural model of the complex, it was an open question whether the disulfide can protect human cells from toxin binding, hereby increasing the biorelevance of testing.

In analogy to the solid-phase test system, concentration dependence and inhibition were first ascertained for VAA binding to cells, here B-lymphoblastic Croco II cells (Fig. 5A, B). The comparative study of the inhibitory potency of galactose and lactose (Fig. 5C) and TDG/DTDG (Fig. 5D) under identical conditions revealed a graded potency, starting with TDG as frontrunner, and underlined the activity of DTDG. Since the glycomic profile and spatial parameters of glycan presentation can differ among various cell lines, we ran the respective assays with a line of another histogenetic origin, *i.e.* colon adenocarcinoma cells, and obtained a similar grading (Fig. 5E, F). In aggregate, these results are in accord with the affinity determinations and prove that DTDG can impair carbohydrate-dependent toxin binding to two types of human cells. Since this lectin's β-trefoil folding is different from the architecture of the β-sandwich-type carbohydrate recognition domain of galectins, which also have extended sites for ligand contacts beyond the galactose core, as inferred by binding assays, NMR spectroscopical monitoring and molecular modelling,[6,11] it is an open question whether DTDG is a galectin ligand. Moreover, intrafamily sequence divergence around the carbohydrate recognition site in galectin genes may lead to differential reactivity. Thus, we tested galectins from each of the three structural subgroups (proto-type with galectins-1 and -7, chimera-type with galectin-3 and tandem-repeat-type with galectins-4 and -8) to address this additional issue.

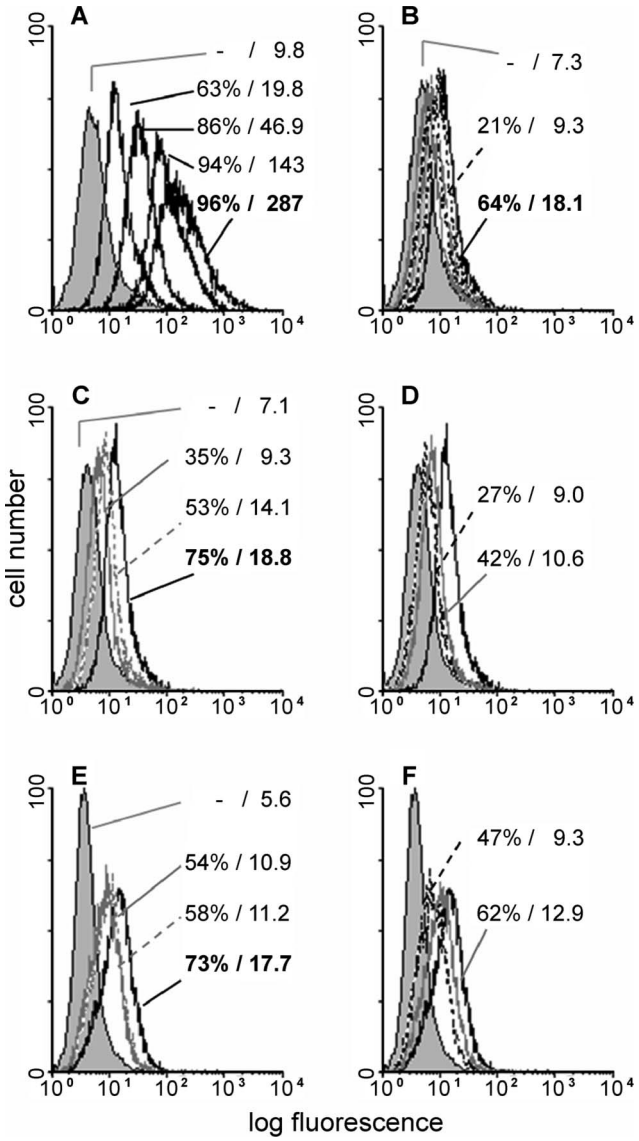

Fig. 5 Semilogarithmic representation of fluorescent surface staining subsequent to VAA binding of cells of the human B-lymphoblastoid line Croco II (A–D; 0.5 μg ml^{-1} VAA in B–D) and of the human colon adenocarcinoma line SW480 (E, F: 2 μg ml^{-1} VAA). The control value of cell positivity by the second-step reagent in the absence of lectin is given as grey-shaded area, the 100%-value (lectin staining in the absence of inhibitor) as thick black line. Numbers characterizing staining (percentage of positive cells/mean fluorescence intensity) in each panel are always given in the order of listing (from top to bottom). A: dependence of staining from increasing the concentration of VAA from 0.2 μg ml^{-1} to 0.5 μg ml^{-1}, 2 μg ml^{-1} and 4 μg ml^{-1}. B: inhibition of VAA-dependent staining by increasing the concentration of lactose from 1 mM to 2 mM, 5 mM and 10 mM (numbers correspond to control value, presence of 10 mM lactose and the 100%-value). C, D: staining parameters in the presence of 5 mM inhibitor (C: lactose, galactose; D: TDG, DTDG). E, F: staining parameters of the colon cancer cells in the presence of 5 mM inhibitor (E: lactose, DTDG; F: TDG, galactose).

Assaying ligand properties on human galectins

The conditions of the solid-phase assay were first optimized for each galectin. The obtained results with TDG were in line with the known reactivity of galectins-1, -3 and -7[6] and extended the reactivity profile to the tandem-repeat-type galectins-4 and -8 (Table 1). When introducing DTDG to the assays, non-uniform

responses at comparatively high concentrations were registered (Table 1). Galectins-1 and -3 were sensitive to DTDG presence, albeit weakly in relation to the plant toxin, whereas the other galectins reacted poorly with the disulfide (Table 1). The use of tumor cell extracts as source for glycoproteins instead of the neoglycoprotein did not alter this result, excluding any ligand-type-related bias. For example, galectin-3 binding was reduced by the three tested compounds with IC_{50}-values of 0.8 mM (TDG), 1.2 mM (lactose) and 4.4 mM (DTDG), as similarly seen with the neoglycoprotein (Table 1).

These results were corroborated by STD NMR spectroscopical series, which revealed a rather weak or no activity for DTDG for the galectins. Guiding model building to explain the negative impact of the disulfide linkage on galectin binding, the STD-based epitope mapping for TDG showed intense signals for the H4, H5 and H6 protons, the characteristic signature for galectin contact (Fig. 3 right). These data, together with the crystal structures of the galectin of toad ovary and human galectin-1 in complex with TDG,[12] provided the input and quality control for molecular modeling studies. Similar to lactose, TDG thus engages both moieties of the disaccharide for binding to galectin-1. This pattern changes due to the presence of the disulfide in the glycosidic linkage. One sugar residue still enters the binding site and maintains the contact pattern, whereas the second would be completely exposed to the solvent, with arrest of the angle of the S–S bond at about 90° (Fig. 6A). The structural constellation remained rather stable over the entire 6-ns period of the MD simulation. Of note, the analysis of the MD trajectories, after superimposition of the two galectin-1/ligand complexes, enabled identification of a water molecule, which could take the place of the OH2 group of TDG in mediating the hydrogen-bonding network with Arg48/Glu71 shown in Fig. 6B. Overall, the disclosed lack of contact building beyond the interacting galactose of the symmetric diglycosyldisulfide will then, apparently, set strict limits to the affinity. Evidently, the disulfide bonding, itself being subject to a conformational arrest, impairs the potential for interacting with galectins.

This impairment was also seen on the level of cell binding, where galectins interact with complex glycans of natural glycoconjugates, as documented by cytofluorimetric analysis with galectin-3 and colon adenocarcinoma cells (Fig. 7A, B) as well as for galectin-4 and pancreatic adenocarcinoma cells (Fig. 7C–F). In the latter case, the apparent strongly negative impact on inhibitory potency was further confirmed by ITC (Fig. 2B). Addition of DTDG to the galectin-4-containing solution triggered only negligible heat generation, comparable to the signal of ligand dilution (Fig. 2B). The titration profiles also highlight the conspicuous reactivity difference to the toxin shown in panel A. Titrations with TDG and galectin-4 as positive control yieled an association constant of 1210 ± 30 M^{-1} (ΔG = –17.53 ± 0.07 kJ mol^{-1}) and estimated enthalpy/entropy values of –39.9 ± 0.8 kJ mol^{-1}/–75 ± 3 J mol^{-1} K^{-1} based on a one-set-of-sites model (assuming two equivalent and independent sites per molecule), and no evidence for cooperativity. Lactose binds similarly with a comparatively lower affinity (K_a = 585 ± 8 M^{-1}; ΔG = –15.74 ± 0.03 kJ mol^{-1}) due to an increased entropic penalty (ΔH = –43 ± 2 kJ mol^{-1}, ΔS = –93 ± 7 J mol^{-1} K^{-1}) (not shown).

Finally, to track down ligand properties of DTDG at a very sensitive level, we performed radiobinding assays to lactose-presenting agarose beads and a surface-presented glycoprotein (asialofibrin films) with iodinated protein using the two galectin-4 domains separately. These experiments will also inform us about the binding properties of the two, structurally distinct domains of galectin-4. Extent of binding of the labelled lectin domains was measured in presence of increasing concentrations of lactose, TDG and DTDG. Apparent association constants were calculated from the plot of the reciprocal of the lectin fraction bound to the ligand *vs.* the inhibitor concentration.[13] A representative plot of data for the C-terminal domain is given in Fig. 8. In relation to the ITC data for the full-length form of galectin-4, the association

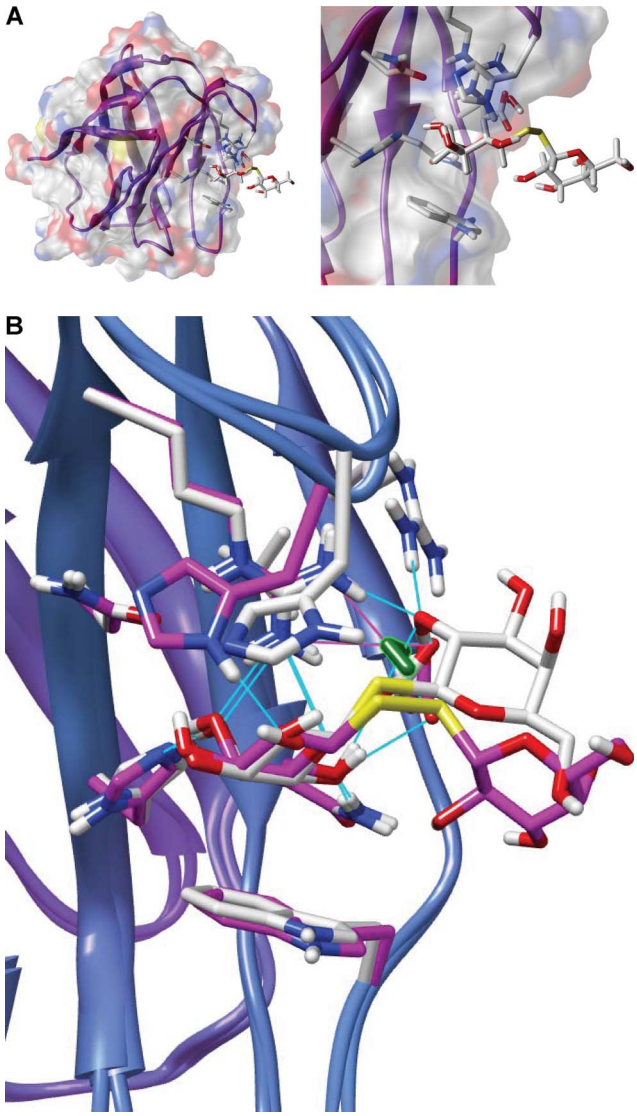

Fig. 6 Illustration of the models of the average structures of the complexes of human galectin-1 with dithiodigalactoside (A) based on MD simulations showing the key intermolecular contacts. Different perspectives in the full and expanded views are offered for the sake of clarity. (B) Superimposition of the complexes with TDG (thiodiglycoside in white) and DTDG (diglycosyldisulfide in magenta), also revealing the presence of the water molecule that, in the second complex, substitutes the OH2 of the second galactose moiety of TDG to mediate a hydrogen-bonding network with Arg48 and Glu71. Intermolecular hydrogen bonds are highlighted with lines.

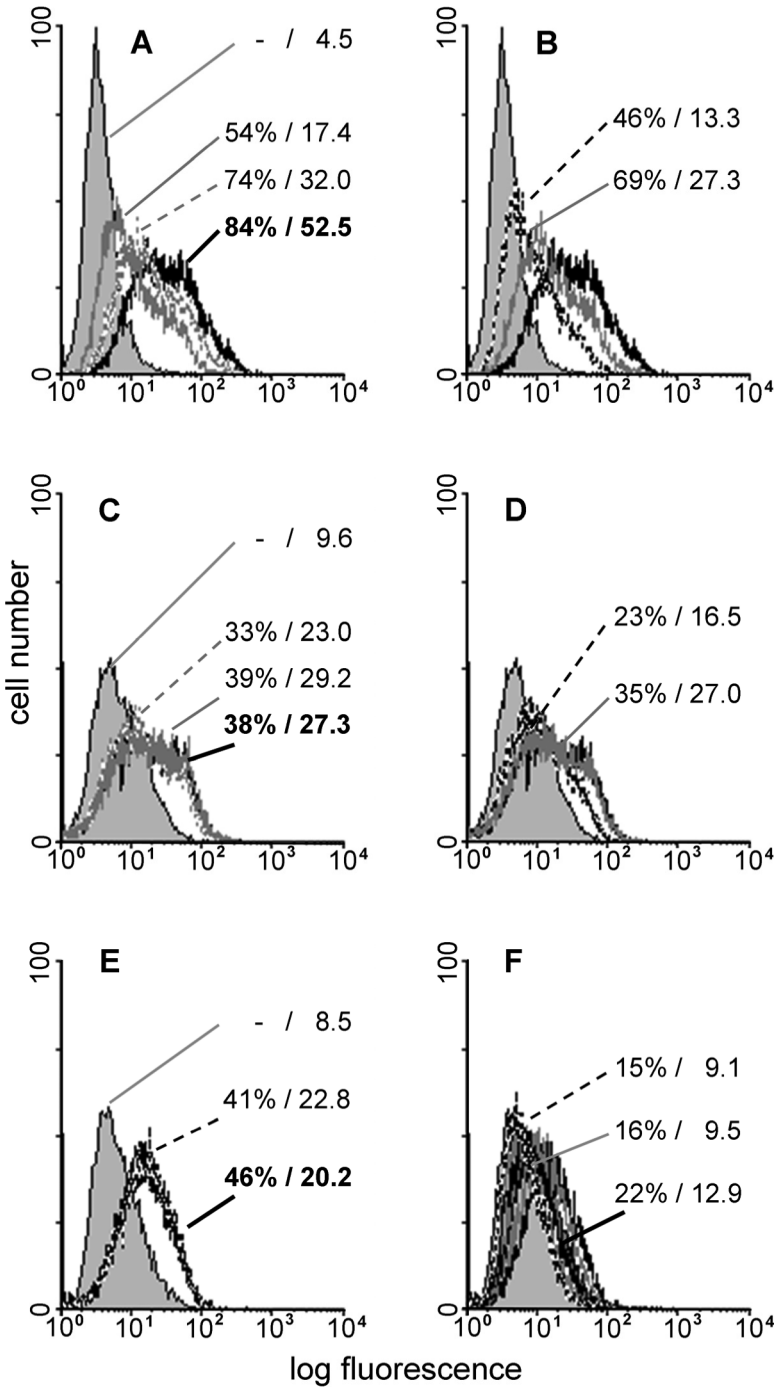

Fig. 7 Semilogarithmic representation of fluorescent surface staining upon binding of galectin-3 (A, B) and galectin-4 (C–F) of cells of the human colon adenocarcinoma line SW480 (A, B) and the pancreatic adenocarcinoma line Capan-1 with functional tumor suppressor $p16^{INK4a}$ (C–F). For details on presentation, please see legend to Fig. 5. A, B: staining parameters in the presence of 2 mM inhibitor for galectin-3 at 10 μg ml^{-1} (A: lactose, galactose; B: TDG, DTDG). C, D: staining parameters in the presence of 2 mM inhibitors for galectin-4 at 20 μg ml^{-1} (C: lactose, galactose; D: TDG, DTDG). E, F: staining parameters in the presence of 20 mM DTDG (E) and in the presence of decreasing concentrations of TDG (F: 20 mM, 10 mM, 5 mM).

constants for lactose were in the same range with values of 300 ± 40 M^{-1} and 440 ± 60 M^{-1} for the N- and C-terminal domains, respectively. Thus, the fit for the one-set-of-sites model of ITC data is attributable to this similarity. The affinity increase for TDG was also determined, with K_a-values of 730 ± 90 M^{-1} and 670 ± 50 M^{-1}, respectively. This set-up enabled to trace even minor DTDG reactivity. By going up to 10 mM DTDG, lectin binding to the matrix-presented ligand was reduced by about 25%, from which an upper limit of the association constant at <30 M^{-1} could be estimated for both domains. Thus, DTDG is definitely only a very weak ligand for galectin-4, on the level of both domains.

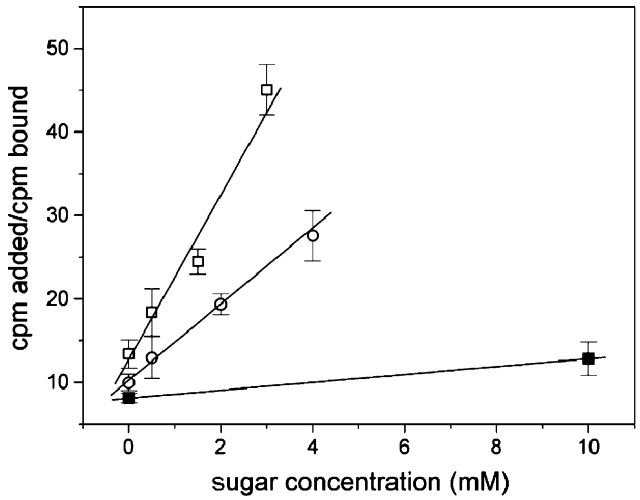

Fig. 8 Inhibitory potency of lactose (○), thiodigalactoside (□) and dithiodigalactoside (■) on the binding of the C-terminal domain of galectin-4 in a solid-phase radioassay. The extent of binding of the ^{125}I-labelled domain to asialofibrin films (100 μg) presented on the plastic microwell surface was measured in the absence and presence of different concentrations of the tested sugar compounds.

Conclusions

Work with dynamic combinatorial thioglycoside libraries had indicated potential for DTDG to react with an AB-type plant toxin.[4d] The results reported here define DTDG as ligand in different biochemical assays, characterize its respective properties in structural terms and document its capacity to protect human cells from toxin binding. The same panel of strategically combined experimental and computational methods delineated a significant difference in reactivity to human galectins, notably with intrafamily grading. Glycosyldisulfides are thus a new substance platform to accomplish selective inhibition of this class of endogenous lectins and a plant AB-type toxin. The computation of a structural model revealed a lack of contact of the second galactose moiety in the case of the disulfide. Exploration of additional substitutions at the 2′- and 3′-positions, *e.g.* 2′-fucosylation,[14] the introduction of anomeric and aglyconic extensions[2g,8,15] and the conjugation to certain scaffolds, *e.g.* starburst glycodendrimers, cyclodextrin, glycocyclophanes or cyclic neoglycopeptides,[16] are routes to further increase the level of affinity and selectivity. This also applies to capitalize on intrafamily differences among galectins, when aiming to block a certain protein in a functional context such as tumor progression or intergalectin competition during growth regulation.[17] Having herewith revealed the bioactivity of the symmetric dithiodigalactoside, it is an emerging question whether the respective selenides, whose conformational flexibility can resemble that of thioglycosides,[18] will be lectin ligands.

Experimental

Materials and general methods

All commercial reagents and solvents were used as received. Chemical reactions were monitored with thin-layer chromatography using precoated silica gel 60 (0.25 mm thickness) plates. Flash column chromatography was performed on silica gel 60 (0.040–0.063 mm). ^{1}H-NMR and ^{13}C-NMR spectra were recorded on a Bruker Avance 400 spectrometer at 400 (100) MHz and/or Bruker Avance DMX 500 at 500 (125) MHz, respectively. Compound **1** was purchased from Sigma.

2,3,4,6-Tetra-*O*-acetyl-1-*S*-acetyl-1-thio-β-D-galactopyranose (adapted from [4b,19a]) (2)[19b]

1,2,3,4,6-Penta-*O*-acetyl-β-D-galactopyranose (**1**) (2 g, 5.13 mmol; please see Scheme 1) and thioacetic acid (1.52 ml, 21.51 mmol) were dissolved in dry CH_2Cl_2 (25 ml) at 0 °C, and $BF_3{\cdot}Et_2O$ (3.889 ml, 31.51 mmol) was added dropwise over a period of 15 min. The reaction mixture was allowed to warm to ambient temperature and stirred under nitrogen protection for 24 h. The reaction mixture was then poured onto ice-cold water, and extracted with CH_2Cl_2. The combined organic layers were successively washed with $NaHCO_3$, water and brine, dried over $MgSO_4$, and filtered. The crude product was purified by column chromatography (eluent: hexane/EtOAc 3 : 1) to give 2,3,4,6-tetra-*O*-acetyl-1-*S*-acetyl-1-thio-β-D-galactopyranose (**2**)[19b] (1.85 g, 4.56 mmol, yield 89%). mp 117 °C. ^{1}H NMR ($CDCl_3$, 500 MHz): δ (ppm) 5.45 (d, 1H, J = 3.4 Hz, H-4), 5.32 (t, 1H, J = 10.1 Hz, H-2), 5.25 (d, 1H, J = 10.2 Hz, H-1), 5.11 (dd, 1H, J = 3.4, 9.8 Hz, H-3), 4.03–4.16 (m, 3H, H-5, H-6, H-6′), 2.39 (s, 3H, SCOCH3), 2.08, 2.03, 2.02, 2.01 (12H, 4 s, 4 OCOCH3); ^{13}C NMR ($CDCl_3$, 125 MHz): δ (ppm) 192.1, 170.3, 170.1, 169.9, 19.5, 80.6, 75.0, 71.9, 67.2, 66.3, 61.2, 30.8, 20.7, 20.6, 20.6, 20.5. MS (ESI): m/z = 429.06 [M + Na^+], $C_{16}H_{22}O_{10}S$; found 429.00.

1-Thio-β-D-galactopyranose sodium salt (3)[19b]

Compound **2** (1.85 g, 4.56 mmol, yield 89%) was dissolved in a MeOH solution (15 ml) of NaOMe (271 mg, 5.02 mmol). The chemical reaction in the resulting mixture quantitatively yielded product **3**. ^{1}H-NMR (500 MHz, D_2O): δ = 4.49 (d, J = 9.1 Hz, 1H, H-1), 3.92 (d, J = 3.6 Hz, 1H, H-4), 3.74 (dd, J = 11.2, 7.6 Hz, 1H, H-6), 3.61–3.69 (m, 2H, H-5, H-6′), 3.58 (dd, J = 9.5, 3.6 Hz, 1H, H-3), 3.31 (t, J = 9.2 Hz, 1H, H-2). ^{13}C NMR (D_2O, 125 MHz): δ (ppm) 85.8, 80.1, 77.4, 75.1, 71.0, 62.7.

1,1′-Dithio-β-D-digalactopyranoside (4)[19c]

Compound **3** (0.2 g, 0.92 mmol) was dissolved in water (3 ml), and a saturated ethanolic solution of iodine was added dropwise until a persistent yellow color appeared in the mixture. The solvent was evaporated, the crude product was dissolved in MeOH and precipitated by the addition of an excess of EtOAc. Filtration of the white solid yielded pure compound **4**[19c] in good yield (0.16 g, 0.41 mmol, yield 89%). The procedure was repeated twice to remove remaining traces of compound **3**. ^{1}H NMR (D_2O, 500 MHz): δ (ppm) 4.54 (d, 2H, J = 9.7 Hz, H-1, H′-1), 3.97 (d, 2H, J = 3.26 Hz, H-4, H′-4), 3.83 (t, 2H, J = 9.7 Hz, H-2, H′-2), 3.72–3.80 (m, 4H, H-5, H′-5, H-6, H′-6), 3.72 (dd, 2H, J = 3.1, 12.3 Hz, H-6′, H′-6′), 3.69 (dd, 2H, J = 3.3, 9.5 Hz, H-3, H′-3); ^{13}C NMR (D_2O, 125 MHz): δ (ppm) 89.9, 79.6, 73.9, 68.8, 68.7, 61.1.

Lectin purification and quality controls

Purification of the lectins started from extracts of dried mistletoe leaves (VAA) and bacterial pellets after recombinant production

(human full-length galectins and the two separate galectin-4 domains) and included affinity chromatography on lactosylated Sepharose 4B, obtained after divinyl sulfone activation, as central step.[20] Purity was routinely ensured by one- and two-dimensional gel electrophoresis and mass spectrometry, quaternary structure by gel filtration and activity by i) haemagglutination using trypsin-treated and glutaraldehyde-fixed rabbit erythrocytes, ii) toxicity tests on human tumor lines (Croco II, SW480) and iii) anoikis assays on a responsive cell line (Capan-1).[21] Biotinylation of the lectins with the N-hydroxysuccinimide ester derivative of biotin (Sigma, Munich, Germany) was performed under activity-preserving conditions and was followed by mass spectrometric product analysis to quantify label incorporation and identify sites of conjugation.[22]

Inhibition spectrophotometric assay

Neoglycoprotein (bovine serum albumin free of contaminating glycoproteins after conjugation of the *p*-isothiocyanatophenyl derivative of lactose[23]) was adsorbed to the surface of microtiter plate wells (0.25 μg/well in 50 μl) from phosphate-buffered saline at 4 °C overnight, and residual sites on the plastic surface for binding proteins were then saturated for 1 h at 37 °C with albumin (100 μl of a 1% solution (w/v); Biomol, Hamburg, Germany). Protein extracts from SW480 colon adenocarcinoma cells were prepared by sonication of cells suspended in 50 mM Tris/HCl buffer (pH 8.0) containing 150 mM NaCl and 1% (v/v) Nonidet P-40. Aliquots of the solution with (glyco)proteins (supernatant after centrifugation; 0.5 μg/well) were kept in microtiter plate wells overnight for coating as described above. Incubation with lectin-containing solution in the absence and presence of tested compounds was performed for 1 h at 37 °C and the extent of lectin binding was spectrophotometrically determined after colorimetric detection of biotin with streptavidin-peroxidase conjugate (Sigma) as described.[23] Assays were routinely run in triplicates in up to six independent series with eight concentrations of sugar, standard deviations not exceeding 13.7%.

Isothermal titration calorimetry

The calorimetric titrations were performed at 25 °C with a Microcal MCS-ITC microcalorimeter (Microcal LLC., Northampton, MA, USA). VAA samples were exhaustively dialyzed against 5 mM sodium phosphate buffer, pH 7.2, containing 0.2 M NaCl (PBS), whereas PBS containing 4 mM β-mercaptoethanol was used for equilibration in the case of human galectin-4. For calorimetric titrations of galectin-4 with DTDG, the reducing agent was excluded from the last dialysis buffer in order to avoid reduction of the glycosyldisulfide. Sugar solutions were prepared using the last dialysis buffer. Titrations were performed by stepwise injections of ligand-containing solution into the reaction cell loaded with the protein solution at concentrations of 117–337.5 μM, depending on the lectin. VAA concentrations were routinely determined using a colorimetric assay ascertained to be applicable for AB toxins, theoretical molar adsorption coefficients were used for galectin-4.[24] The heat developed by ligand dilution was determined separately and subtracted from the total heat produced following each injection. Titration data were analyzed using the Microcal-ITC Origin software. The concentration of the momomer of galectin-4 and of the covalently linked AB heterodimer of VAA was used as input in the fitting procedures.

STD NMR experiments

All experiments were performed at a lectin concentration of 50 μM on a Bruker Avance DRX 500 MHz NMR spectrometer equipped with a 5 mm TXI inverse probe head achieving protein saturation by 40 selective 70 dB Gaussian pulses of 50 ms duration and a total number of 360 (VAA) or 720 (galectins) scans.[8,25] The ligand to protein ratio was set to 80 : 1, competition experiments between lactose and the derivatives were performed up to reaching equimolar concentrations. All details on epitope mapping and competition can be obtained upon request from the authors.

Quantum mechanical methods, partial charges, and molecular mechanics force field

Starting from the geometry of the crystallographic structure of lactose in the PDB file 1GZW,[26] and of TDG in the PDB file 1A78,[12a] we constructed structures for TDG and DTDG, which were subjected to a full geometry optimization by quantum mechanical calculations based on the Gaussian03 program[27] using the B3LYP method and a 6-31G(d) basis set. The resulting wavefunctions were used to calculate electrostatic potential-derived (ESP) charges employing the RESP methodology,[28] as implemented in the Amber 9 suite of programs (http://amber.scripps.edu/). For the calculation of dihedral parameters for the torsional barriers around the bonds involving the S atom in TDG and DTDG we used the methyl derivatives Gal-S-Me and Gal-S-S-Me. These values were calculated so as to reproduce, in the AMBER force field, the energy values calculated *ab initio* in Gaussian03 (keyword SCAN) upon rotation of the bond in 20° steps. The remaining bonded and nonbonded parameters were assigned, by analogy or through interpolation from those already present in the AMBER database, in a way consistent with the Glycam-04 force field for carbohydrates (http://glycam.ccrc.uga.edu), which has been tested widely and used successfully in simulations of the type described herein.

Docking analysis

Docking of TDG and DTDG into the binding sites of VAA[6i] and human galectin-1[26] was based on AutoDock 4.2 application.[29] We first validated AutoDock by testing its ability to predict the lactose-binding mode seen in the crystal structure of human galectin-1 (1GZW). Crystallographic water molecules that were identified as important for binding were kept within the docking calculations. From a preceding conformational analysis, different conformers were selected as starting geometries to be docked. Evaluation of the finally docked structures indicated that AutoDock was able to predict the bound-state conformer. The same protocol was applied to TDG and DTDG: the Lamarckian genetic algorithm (LGA) implemented in AutoDock was used, by randomly changing the torsion angles and overall orientation of the molecule (100 runs with 2 500 000 evaluations and a population size of 150 were selected). The mutation and crossover rates were set to 0.80 and 0.02, respectively, and the maximal number of generations was 27 000; elitism was set to 1 and the local search frequency to 0.06. Search parameters were chosen from those previously

established for docking of carbohydrates, and the grid box was restricted around galectin-1's contact site for lactose. From careful analysis of the docking results, the binding pose with the lowest docking energy was selected as the starting point for performing MD simulations in explicit water. All details on calculations are available upon request.

Molecular dynamics simulations

For each of the two free ligands 6-ns MD simulations were carried out employing the calculated parameters, using Amber 9. Each ligand was placed in a 8 Å-deep truncated octahedral box of explicit TIP3P water molecules. The equilibration phase started with energy minimisation of the solvent, followed by an energy minimisation of the entire system without restraints. The system was then heated up from 10 K to 298 K during 100 ps with weak restraints on the solute (positional restraints to α-carbon atoms), followed by a 100 ps MD simulation at constant temperature and pressure (1 atm), without restrictions. Equilibrated structures were used as starting points for 6-ns production trajectories, performed at constant pressure (1 atm) and temperature (288 K), as in the NMR experiments, controlled by the Langevin thermostat with a collision frequency of 1.0 ps^{-1}. During the simulations, SHAKE algorithm was turned on and applied to all hydrogen atoms. A cut-off of 10 Å for all nonbonded interactions was adopted. An integration time step of 2 fs was employed, and periodic boundaries conditions were applied throughout. During all simulations, the Particle Mesh Ewald (PME) method[30] was used to compute long-range electrostatic interactions. Minimisation, equilibration and production phases were carried out by using the sander module, while analyses of the simulations were performed with ptraj module (http://amber.scripps.edu/). The visualization of trajectories was performed using VMD software (http://www.ks.uiuc.edu/). Data were processed and plotted using R software (http://www.r-project.org/). Concerning the conformational behavior of the ligands during the 6-ns MD simulations, *exo*-anomeric regions were sampled for both thioglycosidic torsions, while ω angle around the C5–C6 bond took the expected gg and gt orientations. The set of charges and parameters described before was employed for the MD simulations of complexes with galectin-1. Starting geometries were selected from docking studies as the poses with the lowest docking energy, in full agreement with the NMR data. 6-ns MD simulations of the sugar/receptor complex were carried out following a protocol identical to that described above for the free ligands.

Inhibition cell assay

Cells of the B-lymphoblastic line Croco II, the colon adenocarcinoma line SW480 and the pancreatic adenocarcinoma line Capan-1 reconstituted for tumor suppressor $p16^{INK4a}$ status were cultured and processed for cell staining in a two-step procedure using a streptavidin/R-phycoerythrin conjugate (Sigma), as described in detail in our previous study on dynamic combinatorial thioglycoside libraries to maintain identical conditions.[4d] Decrease of fluorescent staining (as percentage of positive cells and intensity) served as indicator of the inhibitory capacity of the tested compounds. Up to five series of independent measurements on aliquots of cell suspensions of the same passage were run in triplicates, with standard deviation not exceeding 15.5%.

Inhibition radioassays

The two separate carbohydrate recognition domains of human galectin-4 were radioiodinated using IODO-GEN (Pierce Eurochemie), as described previously.[13] Specific activities of 0.57 and 0.35 mCi/mg were obtained for the N- and C-terminal domains, respectively. These ^{125}I-labelled proteins were first tested for maintained binding capacity and then for optimal test conditions. For the N-domain, the amount of labelled protein bound to agarose beads presenting lactose (Sigma) was measured. Aliquots of 10 µl of sedimented resin were incubated with the ^{125}I-protein-containing solution (15000 cpm) in the absence or presence of different concentrations of test compound (final volume: 50 µl). The buffer used was PBS containing 0.1% Tween-20 and 0.4 mM β-mercaptoethanol. The inhibitory capacity of DTDG was evaluated in parallel experiments carried out in the absence of β-mercaptoethanol. After 2 h at 20 °C with regular shaking, the samples were centrifuged and the radioactivity of the supernatant counted. The C-terminal domain was assayed using 100 µg-asialofibrin films on the surface of plastic microwells essentially as described,[13] except that the plate surface was treated with a 2.5% solution of Tween-20 for 1 h at 37 °C to preclude adsorption of protein and the buffer used was PBS containing 0.1% Tween-20 and 0.4 mM β-mercaptoethanol. Again, the reducing agent was omitted when evaluating the ligand properties of DTDG. For the two systems, *i.e.* lactose-agarose and asialofibrin films, carbohydrate-independent binding was determined in the presence of 0.1 M lactose and subtracted from all measurements.

Acknowledgements

This work has been generously supported by grants CTQ2009-08536, SAF2008-00945, BFU2006-10288 and BFU2009-10052 from the Spanish Ministry, an EC Marie Curie Research Training Network grant (contract no. MRTN-CT-2005-019561), the EC research program GlycoHIT (contract ID 260600), the Verein zur Förderung des biologisch-technologischen Fortschritts in der Medizin e. V. and the CIBER of Respiratory Diseases (CIBERES), an initiative from the Spanish Institute of Health Carlos III (*ISCIII*). We thank Drs B. Friday and S. Namirha for inspiring discussions as well as M. V. López-Moyano for excellent technical assistance.

References

1 H.-J. Gabius, ed. *The Sugar Code. Fundamentals of glycosciences*, Wiley-VCH, Weinheim, 2009.
2 (*a*) F. Schweizer and O. Hindsgaul, *Curr. Opin. Chem. Biol.*, 1999, **3**, 291–298; (*b*) P. M. St. Hilaire and M. Meldal, *Angew. Chem., Int. Ed.*, 2000, **39**, 1162–1179; (*c*) A. Barkley and P. Arya, *Chem.–Eur. J.*, 2001, **7**, 555–563; (*d*) O. Ramström and J.-M. Lehn, *Nat. Rev. Drug Discovery*, 2002, **1**, 26–36; (*e*) S. André, C. E. P. Maljaars, K. M. Halkes, H.-J. Gabius and J. P. Kamerling, *Bioorg. Med. Chem. Lett.*, 2007, **17**, 793–798; (*f*) M. J. Borrok and L. L. Kiessling, *J. Am. Chem. Soc.*, 2007, **129**, 12780–12785; (*g*) S. André, D. Giguère, T. K. Dam, C. F. Brewer, H.-J. Gabius and R. Roy, *New J. Chem.*, 2010, **34**, 2229–2240.

3 (*a*) M. R. Hartley and J. M. Lord, *Biochim. Biophys. Acta*, 2004, **1701**, 1–14; (*b*) H.-J. Gabius, *Crit. Rev. Immunol.*, 2006, **26**, 43–79; (*c*) F. Stirpe and M. G. Batelli, *Cell. Mol. Life Sci.*, 2006, **63**, 1850–1866; (*d*) A. Villalobo, A. Nogales-González and H.-J. Gabius, *Trends Glycosci. Glycotechnol.*, 2006, **18**, 1–37; (*e*) R. Schwartz-Albiez, in *The Sugar Code. Fundamentals of glycosciences*, ed. H.-J. Gabius, Wiley-VCH, Weinheim, 2009, pp. 447–467.

4 (*a*) O. Ramström and J.-M. Lehn, *ChemBioChem*, 2000, **1**, 41–48; (*b*) Z. Pei, R. Larsson, T. Aastrup, H. Anderson, J.-M. Lehn and O. Ramström, *Biosens. Bioelectron.*, 2006, **22**, 42–48; (*c*) T. Hotchkiss, H. B. Kramer, K. J. Doores, D. P. Gamblin, N. J. Oldham and B. G. Davis, *Chem. Commun.*, 2005, 4264–4266; (*d*) S. André, Z. Pei, H.-C. Siebert, O. Ramström and H.-J. Gabius, *Bioorg. Med. Chem.*, 2006, **14**, 6314–6326; (*e*) R. Caraballo, M. Sakulsombat and O. Ramström, *Chem. Commun.*, 2010, **46**, 8469–8471.

5 (*a*) B. Aguilera, J. Jiménez-Barbero and A. Fernandez-Mayoralas, *Carbohydr. Res.*, 1998, **308**, 19–27; (*b*) F. Strino, J.-H. Lii, H.-J. Gabius and P. G. Nyholm, *J. Comput.-Aided Mol. Des.*, 2009, **23**, 845–852.

6 (*a*) A. De Waard, S. Hickman and S. Kornfeld, *J. Biol. Chem.*, 1976, **251**, 7581–7587; (*b*) C. P. Sparrow, H. Leffler and S. H. Barondes, *J. Biol. Chem.*, 1987, **262**, 7383–7390; (*c*) R. Ramkumar, A. Surolia and S. K. Podder, *Biochem. J.*, 1995, **308**, 237–241; (*d*) D. Gupta, M. Cho, R. D. Cummings and C. F. Brewer, *Biochemistry*, 1996, **35**, 15236–15243; (*e*) F. P. Schwarz, H. Ahmed, M. A. Bianchet, L. M. Amzel and G. R. Vasta, *Biochemistry*, 1998, **37**, 5867–5877; (*f*) S. Bharadwaj, H. Kaltner, E. Y. Korchagina, N. V. Bovin, H.-J. Gabius and A. Surolia, *Biochim. Biophys. Acta*, 1999, **1472**, 191–196; (*g*) K. Bachhawat-Sikdar, C. J. Thomas and A. Surolia, *FEBS Lett.*, 2001, **500**, 75–79; (*h*) N. Ahmad, H.-J. Gabius, H. Kaltner, S. André, I. Kuwabara, F.-T. Liu, S. Oscarson, T. Norberg and C. F. Brewer, *Can. J. Chem.*, 2002, **80**, 1096–1104; (*i*) M. Jiménez, S. André, C. Barillari, A. Romero, D. Rognan, H.-J. Gabius and D. Solís, *FEBS Lett.*, 2008, **582**, 2309–2312.

7 (*a*) B. G. Davis, S. J. Ward and P. M. Rendle, *Chem. Commun.*, 2001, 189–190; (*b*) L. Szilágyi, T.-Z. Illyés and P. Herczegh, *Tetrahedron Lett.*, 2001, **42**, 3901–3903; (*c*) L. Szilágyi and O. Varela, *Curr. Org. Chem.*, 2006, **10**, 1745–1770.

8 (*a*) J. P. Ribeiro, S. André, F. J. Cañada, H.-J. Gabius, A. Butera, R. J. Alves and J. Jiménez-Barbero, *ChemMedChem*, 2010, **5**, 415–419; (*b*) J. P. Ribeiro, D. T. Carvalho, S. André, F. J. Cañada, R. J. Alves, H.-J. Gabius and J. Jiménez-Barbero, *R. C. Chimie*, 2011, **14**, 96–101.

9 M. Jiménez, S. André, H.-C. Siebert, H.-J. Gabius and D. Solís, *Glycobiology*, 2006, **16**, 926–937.

10 (*a*) M. Gilleron, H.-C. Siebert, H. Kaltner, C.-W. von der Lieth, T. Kožár, K. M. Halkes, E. Y. Korchagina, N. V. Bovin, H.-J. Gabius and J. F. G. Vliegenthart, *Eur. J. Biochem.*, 1998, **252**, 416–427; (*b*) J. M. Alonso-Plaza, M. A. Canales, M. Jiménez, J. L. Roldan, A. Garcia-Herrero, L. Itturino, J. L. Asensio, F. J. Cañada, A. Romero, H.-C. Siebert, S. André, D. Solís, H.-J. Gabius and J. Jiménez-Barbero, *Biochim. Biophys. Acta*, 2001, **1568**, 225–236; (*c*) M. C. Fernandez-Alonso, F. J. Cañada, D. Solís, X. Cheng, G. Kumaran, S. André, H.-C. Siebert, D. R. Mootoo, H.-J. Gabius and J. Jiménez-Barbero, *Eur. J. Org. Chem.*, 2004, 1604–1613.

11 (*a*) H.-C. Siebert, S. André, S.-Y. Lu, M. Frank, H. Kaltner, J. A. van Kuik, E. Y. Korchagina, N. V. Bovin, E. Tajkhorshid, R. Kaptein, J. F. G. Vliegenthart, C.-W. von der Lieth, J. Jiménez-Barbero, J. Kopitz and H.-J. Gabius, *Biochemistry*, 2003, **42**, 14762–14773; (*b*) A. M. Wu, T. Singh, J.-H. Liu, M. Krzeminski, R. Russwurm, H.-C. Siebert, A. M. J. J. Bonvin, S. André and H.-J. Gabius, *Glycobiology*, 2007, **17**, 165–184; (*c*) M. Krzeminski, T. Singh, S. André, M. Lensch, A. M. Wu, A. M. J. J. Bonvin and H.-J. Gabius, *Biochim. Biophys. Acta*, 2011, **1810**, 150–161.

12 (*a*) M. A. Bianchet, H. Ahmed, G. R. Vasta and L. M. Amzel, *Proteins: Struct., Funct., Genet.*, 2000, **40**, 378–388; (*b*) K. A. Stannard, P. M. Collins, K. Ito, E. M. Sullivan, S. A. Scott, E. Gabutero, I. Darren Grice, P. Low, U. J. Nilsson, H. Leffler, H. Blanchard and S. J. Ralph, *Cancer Lett.*, 2010, **299**, 95–110.

13 (*a*) A. Rivera-Sagredo, D. Solís, T. Díaz-Mauriño, J. Jiménez-Barbero and M. Martín-Lomas, *Eur. J. Biochem.*, 1991, **197**, 217–228; (*b*) D. Solís, A. Romero, H. Kaltner, H.-J. Gabius and T. Díaz-Mauriño, *J. Biol. Chem.*, 1996, **271**, 12744–12748.

14 O. E. Galanina, H. Kaltner, L. S. Khraltsova, N. V. Bovin and H.-J. Gabius, *J. Mol. Recognit.*, 1997, **10**, 139–147.

15 (*a*) R. T. Lee, H.-J. Gabius and Y. C. Lee, *J. Biol. Chem.*, 1992, **267**, 23722–23727; (*b*) R. T. Lee, H.-J. Gabius and Y. C. Lee, *Carbohydr. Res.*, 1994, **254**, 269–276; (*c*) M. Kolympadi, M. Vontanella, C. Venturi, S. André, H.-J. Gabius, J. Jiménez-Barbero and P. Vogel, *Chem.–Eur. J.*, 2009, **15**, 2861–2873.

16 (*a*) S. André, P. C. Ortega, M. A. Perez, R. Roy and H.-J. Gabius, *Glycobiology*, 1999, **9**, 1253–1261; (*b*) S. André, H. Kaltner, T. Furuike, S.-I. Nishimura and H.-J. Gabius, *Bioconjugate Chem.*, 2004, **15**, 87–98; (*c*) R. Leyden, T. Velasco-Torrijos, S. André, S. Gouin, H.-J. Gabius and P. V. Murphy, *J. Org. Chem.*, 2009, **74**, 9010–9026; (*d*) S. André, O. Renaudet, I. Bossu, P. Dumy and H.-J. Gabius, *J. Pept. Sci.*, 2011, **17**, 427–437.

17 (*a*) J. Kopitz, C. von Reitzenstein, S. André, H. Kaltner, J. Uhl, V. Ehemann, M. Cantz and H.-J. Gabius, *J. Biol. Chem.*, 2001, **276**, 35917–35923; (*b*) S. Rorive, N. Belot, C. Decaestecker, F. Lefranc, L. Gordower, S. Micik, C.-A. Maurage, H. Kaltner, M.-M. Ruchoux, A. Danguy, H.-J. Gabius, I. Salmon, R. Kiss and I. Camby, *Glia*, 2001, **33**, 241–255; (*c*) S. Langbein, J. Brade, J. K. Badawi, M. Hatzinger, H. Kaltner, M. Lensch, K. Specht, S. André, U. Brinck, P. Alken and H.-J. Gabius, *Histopathology*, 2007, **51**, 681–690; (*d*) O. Roda, E. Ortíz-Zapater, N. Martínez-Bosch, R. Gutiérrez-Gallego, M. Villa-Perelló, C. Ampurdanés, H.-J. Gabius, S. André, D. Andreu, F. X. Real and P. Navarro, *Gastroenterology*, 2009, **136**, 1379–1390; (*e*) H. Sanchez-Ruderisch, C. Fischer, K. M. Detjen, M. Welzel, A. Wimmel, J. C. Manning, S. André and H.-J. Gabius, *FEBS J.*, 2010, **277**, 3552–3563.

18 F. Strino, J.-H. Lii, C. A. K. Koppisetty, P.-G. Nyholm and H.-J. Gabius, *J. Comput.-Aided Mol. Des.*, 2010, **24**, 1009–1021.

19 (*a*) K. Czifrák and L. Somsák, *Carbohydr. Res.*, 2009, **344**, 269–277; (*b*) R. R. Schmidt and M. Stumpp, *Liebigs Ann. Chem.*, 1983, 1249–1256; (*c*) M. J. Kiefel, R. M. Thomson, M. Radovanovic and M. von Itzstein, *J. Carbohydr. Chem.*, 1999, **18**, 937–959.

20 (*a*) H.-J. Gabius, H. Walzel, S. S. Joshi, J. Kruip, S. Kojima, V. Gerke, H. Kratzin and S. Gabius, *Anticancer Res.*, 1992, **12**, 669–676; (*b*) A. Beer, S. André, H. Kaltner, M. Lensch, S. Franz, K. Sarter, C. Schulze, U. S. Gaipl, P. Kern, M. Herrmann and H.-J. Gabius, *Cytometry, Part A*, 2008, **73A**, 139–147.

21 (*a*) H.-J. Gabius, R. Engelhardt, F. Cramer, R. Bätge and G. A. Nagel, *Cancer Res.*, 1985, **45**, 253–257; (*b*) H.-J. Gabius, F. Darro, M. Remmelink, S. André, J. Kopitz, A. Danguy, S. Gabius, I. Salmon and R. Kiss, *Cancer Invest.*, 2001, **19**, 114–126; (*c*) S. André, H. Sanchez-Ruderisch, H. Nakagawa, M. Buchholz, J. Kopitz, P. Forberich, W. Kemmner, C. Böck, K. Deguchi, K. M. Detjen, B. Wiedenmann, M. von Knebel Doeberitz, T. M. Gress, S.-I. Nishimura, S. Rosewicz and H.-J. Gabius, *FEBS J.*, 2007, **274**, 3233–3256; (*d*) D. Solís, M. J. Maté, M. Lohr, J. P. Ribeiro, L. López-Merino, S. André, E. Buzamet, F. J. Cañada, H. Kaltner, M. Lensch, F. M. Ruiz, G. Haroske, U. Wollina, M. Kloor, J. Kopitz, J. L. Sáiz, M. Menéndez, J. Jiménez-Barbero, A. Romero and H.-J. Gabius, *Int. J. Biochem. Cell Biol.*, 2010, **42**, 1019–1029.

22 (*a*) H.-J. Gabius, B. Wosgien, M. Hendrys and A. Bardosi, *Histochemistry*, 1991, **95**, 269–277; (*b*) D. Kübler, C.-W. Hung, T. K. Dam, J. Kopitz, S. André, H. Kaltner, M. Lohr, J. C. Manning, L. He, H. Wang, A. Middelberg, C. F. Brewer, J. Reed, W.-D. Lehmann and H.-J. Gabius, *Biochim. Biophys. Acta*, 2008, **1780**, 716–722.

23 (*a*) H.-J. Gabius, S. Bodanowitz and A. Schauer, *Cancer*, 1988, **61**, 1125–1131; (*b*) S. André, C. Unverzagt, S. Kojima, M. Frank, J. Seifert, C. Fink, K. Kayser, C.-W. von der Lieth and H.-J. Gabius, *Eur. J. Biochem.*, 2004, **217**, 118–134.

24 M. Jiménez, S. André, H.-J. Gabius and D. Solís, *Anal. Biochem.*, 2000, **284**, 418–420.

25 (*a*) J. Jiménez-Barbero, E. Dragoni, C. Venturi, F. Nannucci, A. Ardá, M. Fontanella, S. André, F. J. Cañada, H.-J. Gabius and C. Nativi, *Chem.–Eur. J.*, 2009, **15**, 10423–10431; (*b*) F. J. Muñoz, J. I. Santos, A. Ardá, S. André, H.-J. Gabius, J. V. Sinisterra, J. Jiménez-Barbero and M. J. Hernáiz, *Org. Biomol. Chem.*, 2010, **8**, 2986–2992.

26 M. F. López-Lucendo, D. Solís, S. André, J. Hirabayashi, K.-i. Kasai, H. Kaltner, H.-J. Gabius and A. Romero, *J. Mol. Biol.*, 2004, **343**, 957–970.

27 *Gaussian 03*, Revision C.02, M. J. Frisch, G. W. Trucks, H. B. Schlegel, G. E. Scuseria, M. A. Robb, J. R. Cheeseman, J. A. Montgomery, Jr., T. Vreven, K. N. Kudin, J. C. Burant, J. M. Millam, S. S. Iyengar, J. Tomasi, V. Barone, B. Mennucci, M. Cossi, G. Scalmani, N. Rega, G. A. Petersson, H. Nakatsuji, M. Hada, M. Ehara, K. Toyota, R. Fukuda, J. Hasegawa, M. Ishida, T. Nakajima, Y. Honda, O. Kitao, H. Nakai, M. Klene, X. Li, J. E. Knox, H. P. Hratchian, J.

B. Cross, V. Bakken, C. Adamo, J. Jaramillo, R. Gomperts, R. E. Stratmann, O. Yazyev, A. J. Austin, R. Cammi, C. Pomelli, J. W. Ochterski, P. Y. Ayala, K. Morokuma, G. A. Voth, P. Salvador, J. J. Dannenberg, V. G. Zakrzewski, S. Dapprich, A. D. Daniels, M. C. Strain, O. Farkas, D. K. Malick, A. D. Rabuck, K. Raghavachari, J. B. Foresman, J. V. Ortiz, Q. Cui, A. G. Baboul, S. Clifford, J. Cioslowski, B. B. Stefanov, G. Liu, A. Liashenko, P. Piskorz, I. Komaromi, R. L. Martin, D. J. Fox, T. Keith, M. A. Al-Laham, C. Y. Peng, A. Nanayakkara, M. Challacombe, P. M. W. Gill, B. Johnson, W. Chen, M. W. Wong, C. Gonzalez and J. A. Pople, Gaussian, Inc., Wallingford CT, 2004.

28 I. Bayly, P. Cieplak, W. Cornell and P. Kollman, *J. Phys. Chem.*, 1993, **97**, 10269–10280.

29 G. M. Morris, D. S. Goodsell, R. S. Halliday, R. Huey, W. E. Hart, R. K. Belew and A. J. Olson, *J. Comput. Chem.*, 1998, **19**, 1639–1662.

30 T. A. Darden, D. York and L. G. Pedersen, *J. Chem. Phys.*, 1993, **98**, 10089–10092.